Medical Image Processing Using Transforms

Hongmei Zhu, Ph.D
Department of Mathematics & Statistics
York University
hmzhu@yorku.ca

Outlines

- Image Quality
- Gray value transforms
- Histogram processing
- Filters in image space
- Filters in Fourier space
- Filters in Time-frequency space

5. Filters in Fourier space

5.1. The Fourier transforms

- In 1807, his introductory manuscript “Theory of the propagation of heat in solid bodies”
- In 1822, published "Theacuteorie analytique de la chaleur"

$$u_t = k u_{xx}$$

- Established the mathematical theory of heat diffusion
- Introduced the representation of a function as a series of sines and cosines known as Fourier series

Elena Prestini: evolution of applied harmonic analysis (2004)

The Fourier Transform (1807)

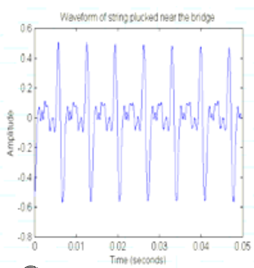

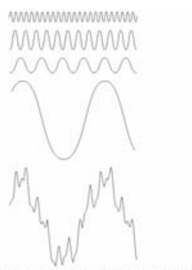

The Fourier Transform

$$f(x) \xrightarrow{\text{Fourier transform}} F(u) = \int_{-\infty}^{+\infty} f(x)\, exp(-j2\pi ux)\, dx$$

$$f(x) = \int_{-\infty}^{+\infty} F(u)\, exp(j2\pi ux)\, du \xleftarrow{\text{Inverser Fourier Transform}} F(u)$$

Joseph Fourier

The Fourier Transform

The FT of a function f(t) is in general complex:

$$F(u) = Re(u) + j\,Im(u)$$

Fourier spectrum: $|F(u)| = \sqrt{Re^2(u) + Im^2(u)}$

Power spectrum (or spectral density): $|F(u)|^2$

Phase angle: $\phi(u) = tan^{-1}\left(\frac{Im(u)}{Re(u)}\right)$

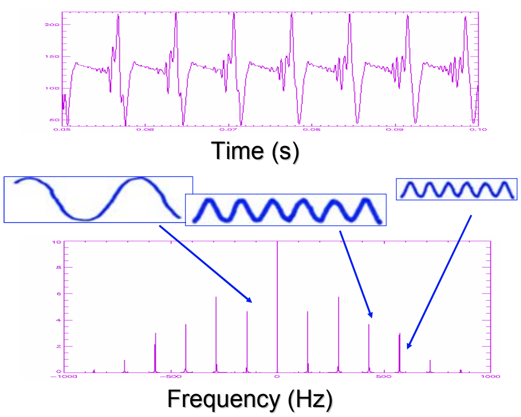

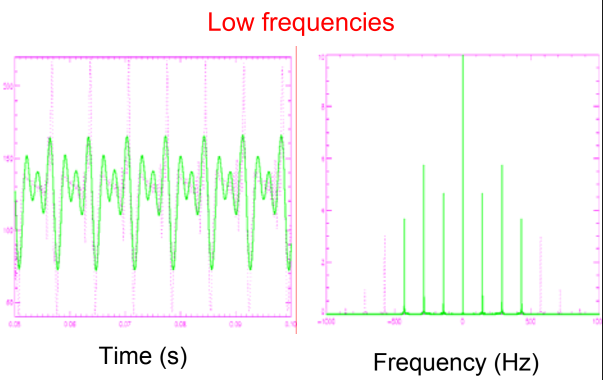

High frequencies

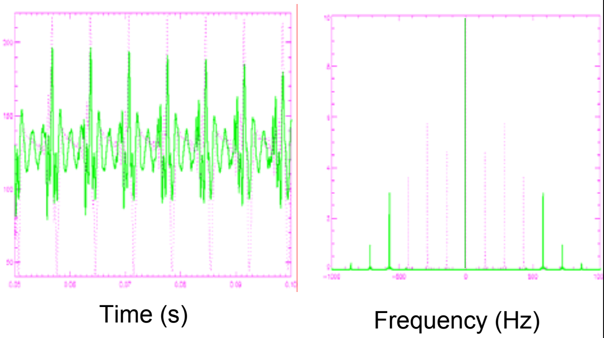

Rectangular function and Sinc

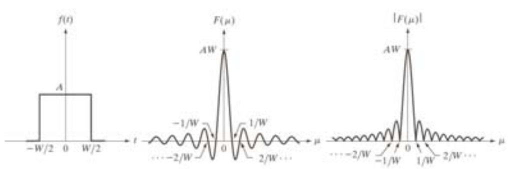

FIGURE 4.4 (a) A simple function; (b) its Fourier transform; and (c) the spectrum. All functions extend to infinity in both directions.

$$\Pi(x) \longleftrightarrow sinc(\pi u)$$

Gaussian and Gaussian

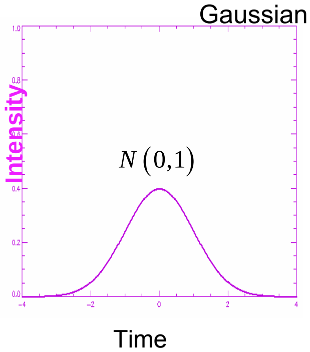

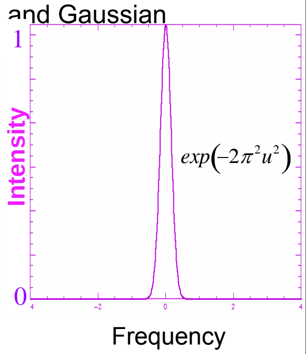

$$exp(-\pi x^2) \longleftrightarrow exp(-\pi u^2)$$

Comb and Comb

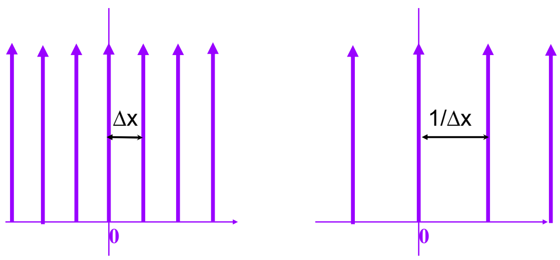

Time

Frequency

$$\frac{1}{\Delta x} comb\left(\frac{x}{\Delta x}\right) \longleftrightarrow comb\left(\frac{u}{\Delta u}\right)$$

Sampling

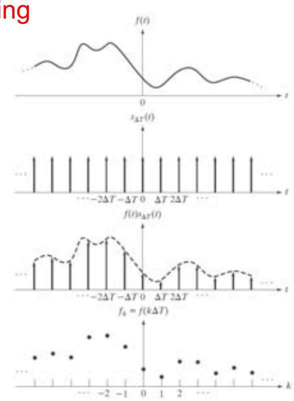

a b c d

FIGURE 4.5 (a) A continuous function. (b) Train of impulses used to model the sampling process. (c) Sampled function formed as the product of (a) and (b). (d) Sample values obtained by integration and using the sifting property of the impulse. (The dashed line in (c) is shown for reference. It is not part of the data.)

YORK U UNIVERSITÉ UNIVERSITY

Some Fourier Properties

Scaling: $h(ax) \longleftrightarrow \frac{1}{|a|} H\left(\frac{u}{a}\right)$

Shifting: $h(x - x_0) \longleftrightarrow H(u)e^{-j2\pi u x_0}$

$h(x)e^{j2\pi u_0 x} \longleftrightarrow H(u - u_0)$

Convolution: $h_1(x) \otimes h_2(x) \longleftrightarrow H_1(u)H_2(u)$

$h_1(x)h_2(x) \longleftrightarrow H_1(u) \otimes H_2(u)$

Convolution Theorem

Definition - Convolution:

$$h_1(x) \otimes h_2(x) \equiv \int_{-\infty}^{+\infty} h_1(\tau) h_2(x-\tau) d\tau$$

Property:

$$h_1 \otimes h_2 = h_2 \otimes h_1$$

16

Fields, 08, HmZhu

Convolution with impluse function

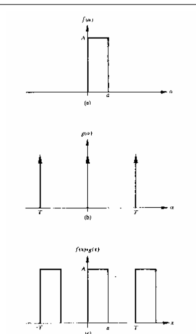

17

Fields, 08, HmZhu

Convolution= Blurring

Convolving a signal with a smooth weighting function can be used to smooth a signal

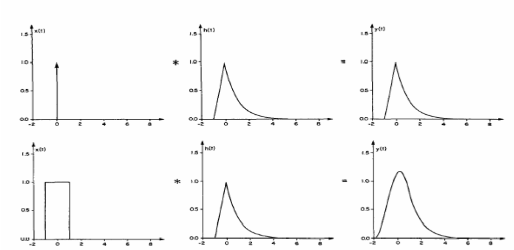

Fig. 2.4: The results of convolving an impulse response with an impulse (top) and a square pulse (bottom) are shown here.

What happens in 2D?

The 2D Fourier Transform

Fields, 08, HmZhu

The 2D Fourier Transform

$$F(k_x, k_y) = \int_{-\infty}^{+\infty}\int_{-\infty}^{+\infty} f(x,y) e^{-j2\pi k_x x}\, dx \cdot e^{-j2\pi k_y y}\, dy$$

$$\updownarrow$$

$$f(x,y) = \int_{-\infty}^{+\infty}\int_{-\infty}^{+\infty} F(k_x, k_y) e^{j2\pi k_x x}\, dk_x\, e^{j2\pi k_y y} dk_y$$

Fields, 08, HmZhu

20

Review of Fourier Theory

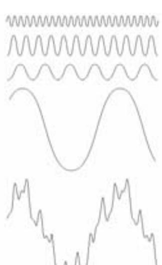

FIGURE 4.1 The function at the bottom is the sum of the four functions above it. Fourier's idea in 1807 that periodic functions could be represented as a weighted sum of sines and cosines was met with skepticism.

21

What are Spatial Frequencies?

FT

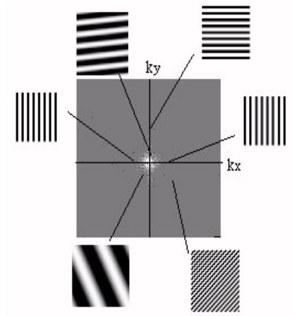

Image

Fourier Spectrum

What's wrong?

FT

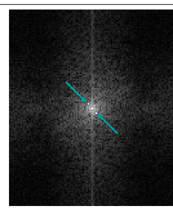

What happened to the image?

Incorrect Fourier spectra

Low Spatial Frequencies

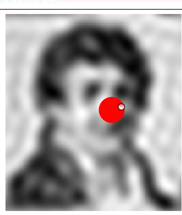

FT

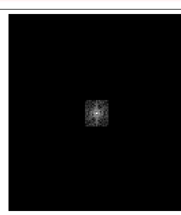

Basic structure of an Image

Low frequencies

High Spatial Frequencies

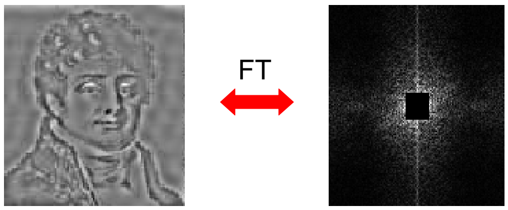

Edges of an image

High frequencies

Amplitude

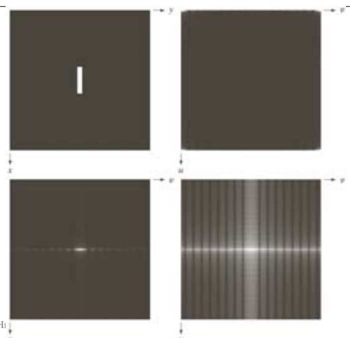

a b
c d

FIGURE 4.24 (a) Image. (b) Spectrum showing bright spots in the four corners. (c) Centered spectrum. (d) Result showing increased detail after a log transformation. The zero crossings of the spectrum are closer in the vertical direction because the rectangle in (a) is longer in that direction. The coordinate convention used throughout the book places the origin of the spatial and frequency domains at the top left.

Amplitude

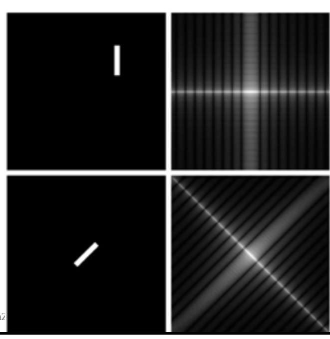

a b
c d

FIGURE 4.25 (a) The rectangle in Fig. 4.24(a) translated, and (b) the corresponding spectrum. (c) Rotated rectangle, and (d) the corresponding spectrum. The spectrum corresponding to the translated rectangle is identical to the spectrum corresponding to the original image in Fig. 4.24(a).

Phase

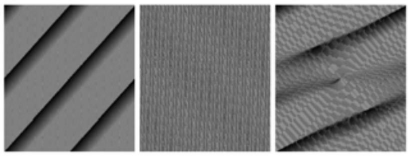

a b c

FIGURE 4.26 Phase angle array corresponding (a) to the image of the centered rectangle in Fig. 4.24(a), (b) to the translated image in Fig. 4.25(a), and (c) to the rotated image in Fig. 4.25(c).

28

Fields, 08, HmZhu

Amplitude and Phase

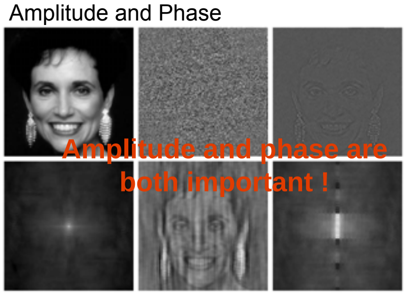

a b c
d e f

FIGURE 4.27 (a) Woman. (b) Phase angle. (c) Woman reconstructed using only the phase angle. (d) Woman reconstructed using only the spectrum. (e) Reconstruction using the phase angle corresponding to the woman and the spectrum corresponding to the rectangle in Fig. 4.24(a). (f) Reconstruction using the phase of the rectangle and the spectrum of the woman.

Basic properties still hold

TABLE 4.3 Summary of DFT pairs. The closed-form expressions in 12 and 13 are valid only for continuous variables. They can be used with discrete variables by sampling the closed-form, continuous expressions.

Name	DFT Pairs
1) Symmetry properties	See Table 4.1
2) Linearity	$af_1(x, y) + bf_2(x, y) \Leftrightarrow aF_1(u, v) + bF_2(u, v)$
3) Translation (general)	$f(x, y)e^{j2\pi(u_0x/M + v_0y/N)} \Leftrightarrow F(u - u_0, v - v_0)$ $f(x - x_0, y - y_0) \Leftrightarrow F(u, v)e^{-j2\pi(ux_0/M + vy_0/N)}$
4) Translation to center of the frequency rectangle, $(M/2, N/2)$	$f(x, y)(-1)^{x+y} \Leftrightarrow F(u - M/2, v - N/2)$ $f(x - M/2, y - N/2) \Leftrightarrow F(u, v)(-1)^{u+v}$
5) Rotation	$f(r, \theta + \theta_0) \Leftrightarrow F(\omega, \varphi + \theta_0)$ $x = r\cos\theta \quad y = r\sin\theta \quad u = \omega\cos\varphi \quad v = \omega\sin\varphi$
6) Convolution theorem[†]	$f(x, y) \star h(x, y) \Leftrightarrow F(u, v)H(u, v)$ $f(x, y)h(x, y) \Leftrightarrow F(u, v) \star H(u, v)$

(Continued)

30

Fields, 08, HmZhu

Basic properties still hold

Name	DFT Pairs
7) Correlation theorem[†]	$f(x,y) \star h(x,y) \Leftrightarrow F^*(u,v)H(u,v)$ $f^*(x,y)h(x,y) \Leftrightarrow F(u,v) \star H(u,v)$
8) Discrete unit impulse	$\delta(x,y) \Leftrightarrow 1$
9) Rectangle	$\text{rect}[a,b] \Leftrightarrow ab\frac{\sin(\pi ua)}{(\pi ua)}\frac{\sin(\pi vb)}{(\pi vb)}e^{-j\pi(ua+vb)}$
10) Sine	$\sin(2\pi u_0 x + 2\pi v_0 y) \Leftrightarrow$ $j\frac{1}{2}\left[\delta(u+Mu_0, v+Nv_0) - \delta(u-Mu_0, v-Nv_0)\right]$
11) Cosine	$\cos(2\pi u_0 x + 2\pi v_0 y) \Leftrightarrow$ $\frac{1}{2}\left[\delta(u+Mu_0, v+Nv_0) + \delta(u-Mu_0, v-Nv_0)\right]$
The following Fourier transform pairs are derivable only for continuous variables, denoted as before by t and z for spatial variables and by μ and ν for frequency variables. These results can be used for DFT work by sampling the continuous forms.	
12) *Differentiation* (The expressions on the right assume that $f(\pm\infty, \pm\infty) = 0$.)	$\left(\frac{\partial}{\partial t}\right)^m\left(\frac{\partial}{\partial z}\right)^n f(t,z) \Leftrightarrow (j2\pi\mu)^m(j2\pi\nu)^n F(\mu,\nu)$ $\frac{\partial^m f(t,z)}{\partial t^m} \Leftrightarrow (j2\pi\mu)^m F(\mu,\nu); \frac{\partial^n f(t,z)}{\partial z^n} \Leftrightarrow (j2\pi\nu)^n F(\mu,\nu)$
13) *Gaussian*	$A2\pi\sigma^2 e^{-2\pi^2\sigma^2(t^2+z^2)} \Leftrightarrow Ae^{-(\mu^2+\nu^2)/2\sigma^2}$ (A is a constant)

[†] Assumes that the functions have been extended by zero padding. Convolution and correlation are associative, commutative, and distributive.

MR Image Reconstruction

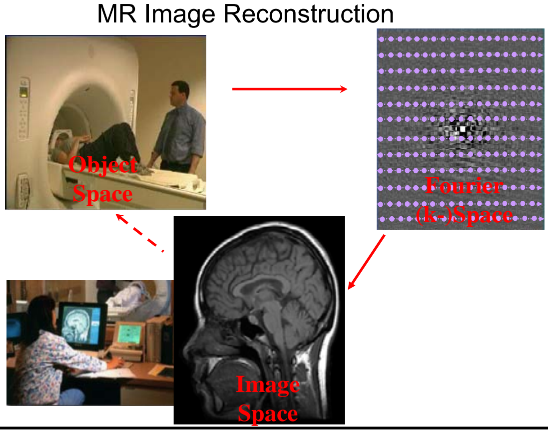

The 1D Discrete FT

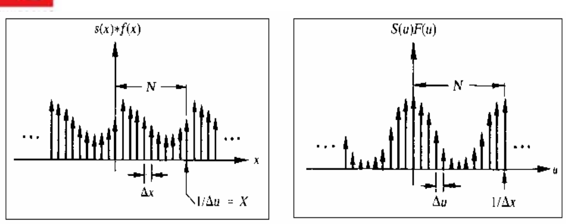

Object space and Fourier space is kind of "inverse" relationship

The 2D Discrete FT

K extend

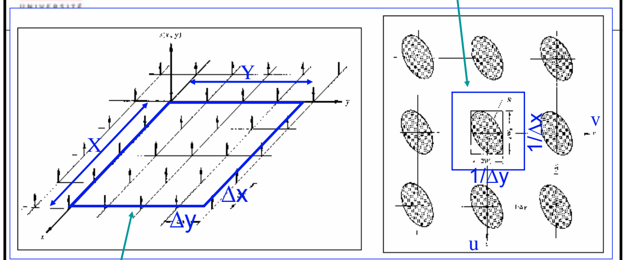

Field of View (FOV)

$$\Delta u = \frac{1}{X} \qquad \Delta v = \frac{1}{Y}$$

Sampling

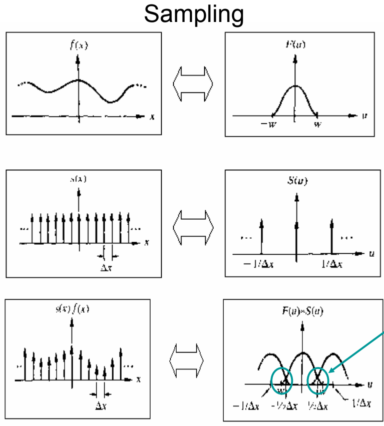

aliasing

Example: Spatial Aliasing

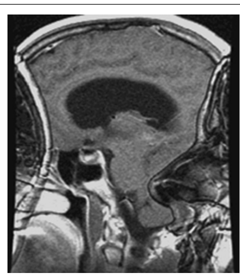

MRI

Nyquist Sampling Criterion

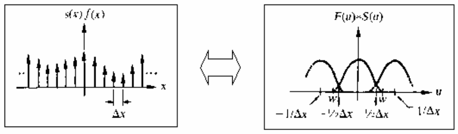

To avoid aliasing, $\frac{1}{2\Delta x} \geq w \quad i.e., \quad \Delta x \leq \frac{1}{2w}$

w: Nyquist frequency   2w: Nyquist rate

That is, the sampling rate needs to be at least twice the max frequency of the function: $\frac{1}{\Delta x} \geq 2w$

Infinite Sampling

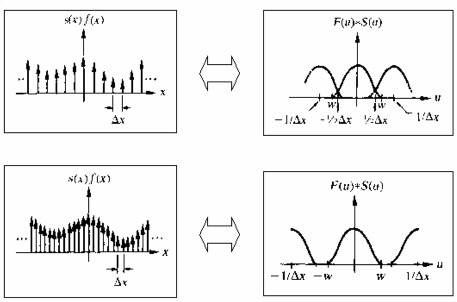

How much data is needed ?

Shannon Sampling Theorem

If h(t) is a band-limited continuous function,
i.e. there is a finite positive w, such that
H(u) = 0 for |u| > w
then h(t) can completely recover from samples whose spacing satisfies Nyquist criterion

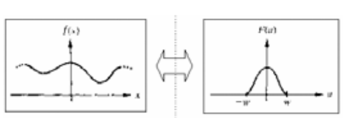

Warning: Using DFT allows us to perform convolution, but the discrete functions are treated as periodic, with a periodic equal to the length of the functions. Wrap-around error could happen.

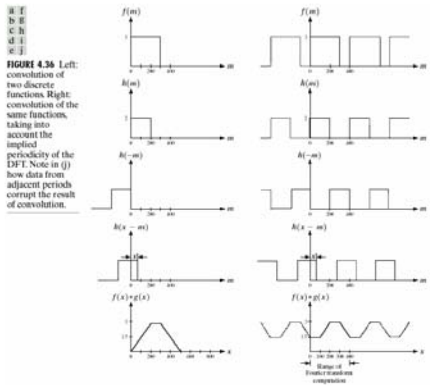

Solution: Assume that f and h consist of A and B points, respectively. We append zeros to both so that they have the identical periods P >= A+B - 1.

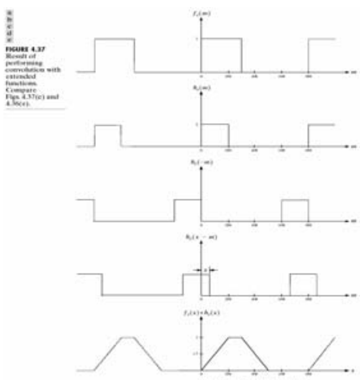

Solution: We zero-extends f(x, y) and h(x, y) so that both have size of P x Q where P >= A+C - 1 and Q >= B+D-1.

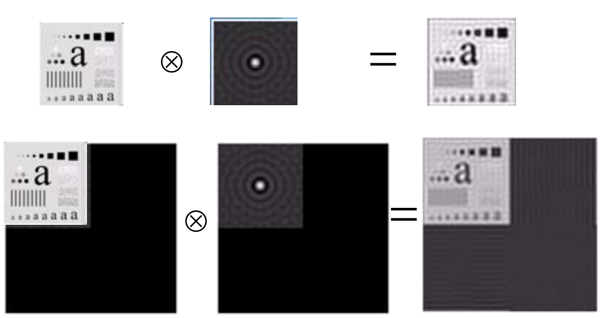

5. Filters in Fourier space

5.2. Filters in Fourier space

Fields, 08, HmZhu

H(u, v) is called filter or filter transfer function, which suppresses certain frequencies while leaving the others unchanged.

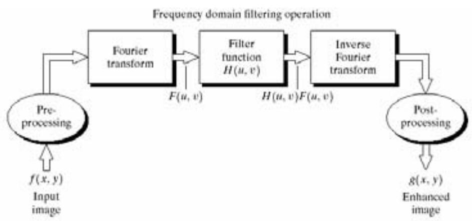

FIGURE 4.5 Basic steps for filtering in the frequency domain.

$$f(x,y)\otimes h(x,y)\Leftrightarrow F(u,v)H(u,v)$$

Example

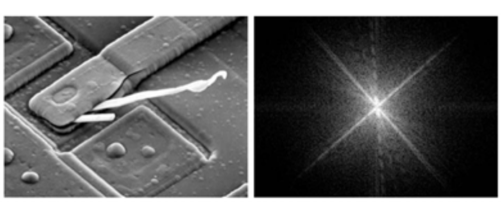

a b

FIGURE 4.29 (a) SEM image of a damaged integrated circuit. (b) Fourier spectrum of (a). (Original image courtesy of Dr. J. M. Hudak, Brockhouse Institute for Materials Research, McMaster University, Hamilton, Ontario, Canada.)

45

Fields, 08, HmZhu

Low pass filters:

attenuates high freq. while passing low freq (smoothing, blurring)

High pass filters:

attenuates low freq while passing high freq (sharpening)

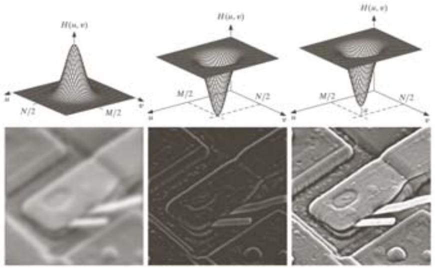

FIGURE 4.31 Top row: frequency domain filters. Bottom row: corresponding filtered images obtained using Eq. (4.7-1). We used $a = 0.85$ in (c) to obtain (f) (the height of the filter itself is 1). Compare (f) with Fig. 4.29(a).

Low pass filters

TABLE 4.4
Lowpass filters. D_0 is the cutoff frequency and n is the order of the Butterworth filter.

Ideal	Butterworth	Gaussian
$H(u,v) = \begin{cases} 1 & \text{if } D(u,v) \le D_0 \\ 0 & \text{if } D(u,v) > D_0 \end{cases}$	$H(u,v) = \dfrac{1}{1 + [D(u,v)/D_0]^{2n}}$	$H(u,v) = e^{-D^2(u,v)/2D_0^2}$

Low pass filters

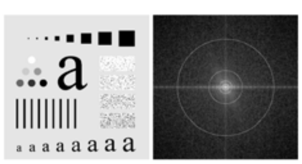

FIGURE 4.41 (a) Test pattern of size 688 × 688 pixels, and (b) its Fourier spectrum. The spectrum is double the image size due to padding but is shown in half size so that it fits in the page. The superimposed circles have radii equal to 10, 30, 60, 160, and 460 with respect to the full-size spectrum image. These radii enclose 87.0, 93.1, 95.7, 97.8, and 99.2% of the padded image power, respectively.

Ideal Low Pass Filter

a b c

FIGURE 4.40 (a) Perspective plot of an ideal lowpass-filter transfer function. (b) Filter displayed as an image. (c) Filter radial cross section.

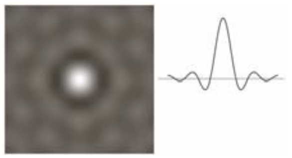

a b

FIGURE 4.43 (a) Representation in the spatial domain of an ILPF of radius 5 and size 1000 × 1000. (b) Intensity profile of a horizontal line passing through the center of the image.

Ideal low pass filter

a b
c d
e f

FIGURE 4.42 (a) Original image. (b)-(f) Results of filtering using ILPFs with cutoff frequencies set at radii values 10, 30, 60, 160, and 460, as shown in Fig. 4.41(b). The power removed by these filters was 13, 6.9, 4.3, 2.2, and 0.8% of the total, respectively.

Fields, 08, HmZhu

50

Butterworth low pass filters

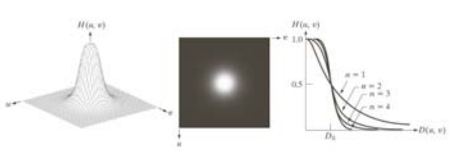

a b c

FIGURE 4.44 (a) Perspective plot of a Butterworth lowpass-filter transfer function. (b) Filter displayed as an image. (c) Filter radial cross sections of orders 1 through 4.

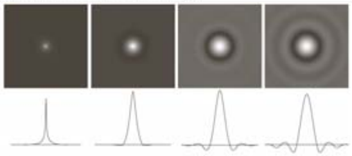

a b c d

FIGURE 4.46 (a)-(d) Spatial representation of BLPFs of order 1, 2, 5, and 20, and corresponding intensity profiles through the center of the filters (the size in all cases is 1000 × 1000 and the cutoff frequency is 5). Observe how ringing increases as a function of filter order.

Ideal Butterworth

Gaussian low pass filters

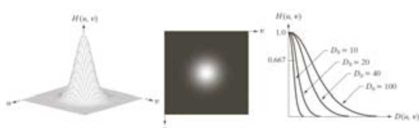

a b c
FIGURE 4.47 (a) Perspective plot of a GLPF transfer function. (b) Filter displayed as an image. (c) Filter radial cross sections for various values of D_0.

Ideal Butterworth Gaussian

High pass filters

$$H_{HP}(u,v) = 1 - H_{LP}(u,v)$$

TABLE 4.5
Highpass filters. D_0 is the cutoff frequency and n is the order of the Butterworth filter.

Ideal	Butterworth	Gaussian
$H(u,v) = \begin{cases} 0 & \text{if } D(u,v) \le D_0 \\ 1 & \text{if } D(u,v) > D_0 \end{cases}$	$H(u,v) = \dfrac{1}{1 + [D_0/D(u,v)]^{2n}}$	$H(u,v) = 1 - e^{-D^2(u,v)/2D_0^2}$

High pass filters

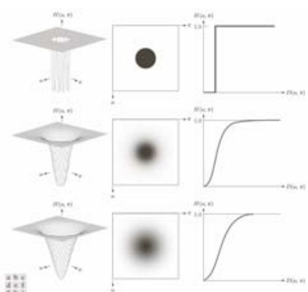

FIGURE 4.52 Top row: Perspective plot, image representation, and cross section of a typical ideal highpass filter. Middle and bottom rows: The same sequence for typical Butterworth and Gaussian highpass filters.

Spatial representations of the high pass filters

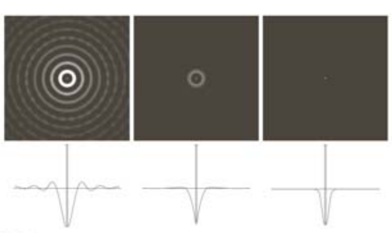

FIGURE 4.53 Spatial representation of typical (a) ideal, (b) Butterworth, and (c) Gaussian frequency domain highpass filters, and corresponding intensity profiles through their centers.

a b c

FIGURE 4.54 Results of highpass filtering the image in Fig. 4.41(a) using an IHPF with D_0 = 30, 60, and 160.

a b c

FIGURE 4.55 Results of highpass filtering the image in Fig. 4.41(a) using a BHPF of order 2 with D_0 = 30, 60, and 160, corresponding to the circles in Fig. 4.41(b). These results are much smoother than those obtained with an IHPF.

a b c

FIGURE 4.56 Results of highpass filtering the image in Fig. 4.41(a) using a GHPF with D_0 = 30, 60, and 160, corresponding to the circles in Fig. 4.41(b). Compare with Figs. 4.54 and 4.55.

YORK UNIVERSITÉ UNIVERSITY

An example of high pass filter

a b c

FIGURE 4.57 (a) Thumb print. (b) Result of highpass filtering (a). (c) Result of thresholding (b). (Original image courtesy of the U.S. National Institute of Standards and Technology.)

YORK UNIVERSITÉ UNIVERSITY

Unshark masking and High-frequency emphasis filter

The mask in the unsharp masking can be defined as

$$g_{mask}(x,y) = f(x,y) - f_{LP}(x,y)$$

where $f_{LP}(x,y) = \mathbb{F}^{-1}\left[H_{LP}(u,v)F(u,v)\right]$.

Then the final filtered image can be expressed as

$$g(x,y) = f(x,y) + k * g_{mask}(x,y)$$

$$= \mathbb{F}^{-1}\left\{\left[1 + k * H_{HP}(u,v)\right]F(u,v)\right\}$$

More general formulation of the high-frequency emphasis filtering

$$g(x,y) = \mathbb{F}^{-1}\left\{\left[k_1 + k_2 * H_{HP}(u,v)\right]F(u,v)\right\}$$

where $k_1, k_2 \geq 0$.

High-frequency emphasis filter

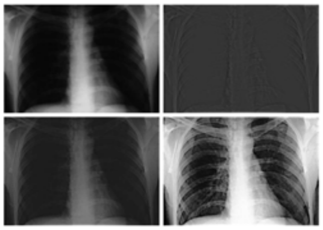

a b
c d

FIGURE 4.59 (a) A chest X-ray image. (b) Result of highpass filtering with a Gaussian filter. (c) Result of high-frequency-emphasis filtering using the same filter. (d) Result of performing histogram equalization on (c). (Original image courtesy of Dr. Thomas R. Gest, Division of Anatomical Sciences, University of Michigan Medical School.)

Fields, 08, HmZhu

61

Bandreject filters

TABLE 4.6
Bandreject filters. W is the width of the band, D is the distance $D(u, v)$ from the center of the filter, D_0 is the cutoff frequency, and n is the order of the Butterworth filter. We show D instead of $D(u, v)$ to simplify the notation in the table.

Ideal	Butterworth	Gaussian
$H(u, v) = \begin{cases} 0 & \text{if } D_0 - \frac{W}{2} \le D \le D_0 + \frac{W}{2} \\ 1 & \text{otherwise} \end{cases}$	$H(u, v) = \dfrac{1}{1 + \left[\dfrac{DW}{D^2 - D_0^2}\right]^{2n}}$	$H(u, v) = 1 - e^{-\left[\frac{D^2 - D_0^2}{DW}\right]^2}$

Fields, 08, HmZhu

62

An Example of Bandreject Filter

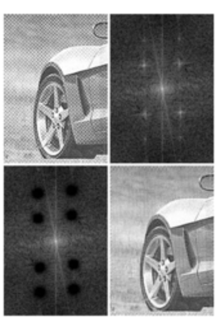

a b
c d

FIGURE 4.64
(a) Sampled newspaper image showing a moiré pattern.
(b) Spectrum.
(c) Butterworth notch reject filter multiplied by the Fourier transform.
(d) Filtered image.

Fields, 08, HmZhu

63

5. Filters in Fourier space

5.3. Deconvolution

redefine THE POSSIBLE

Fields, 08, HmZhu

Image restoration and reconstruction

FIGURE 5.1 A model of the image degradation/restoration process.

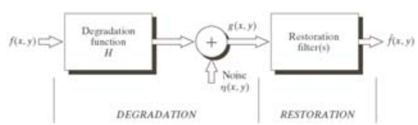

The measured image can be considered as

$$g(x,y) = h(x,y) \otimes f(x,y) + n(x,y)$$

$\downarrow$ FT

$$G(u,v) = H(u,v)F(u,v) + N(u,v)$$

Degraded images

a b
c d

FIGURE 5.25 Illustration of the atmospheric turbulence model. (a) Negligible turbulence. (b) Severe turbulence, $k = 0.0025$. (c) Mild turbulence, $k = 0.001$. (d) Low turbulence, $k = 0.00025$. (Original image courtesy of NASA.)

Inverse filter

The measured image can be considered as

$$g(x,y) = h(x,y) \otimes f(x,y) + n(x,y)$$

$$\downarrow \text{FT}$$

$$G(u,v) = H(u,v)F(u,v) + N(u,v)$$

Given the Fourier response of the degradating function $H(u,v)$, the true image can be estimated by

$$\tilde{F}(u,v) = \frac{G(u,v)}{H(u,v)} = F(u,v) + \frac{N(u,v)}{H(u,v)}$$

Inverse filter

a b
c d
FIGURE 5.27 Restoring Fig. 5.25(b) with Eq. (5.7-1). (a) Result of using the full filter. (b) Result with H cut off outside a radius of 40; (c) outside a radius of 70; and (d) outside a radius of 85.

Wiener filter (1942)

The Wiener filter aims to find an estimate to the true image by minimizing their mean square error.
In the Fourier domain, the spectrum of the estimated image is

$$\tilde{F}(u,v) = \left[\frac{H^*(u,v)}{|H(u,v)|^2 + \frac{|N(u,v)|^2}{|F(u,v)|^2}} \right] G(u,v)$$

$$\approx \left[\frac{1}{H(u,v)} \frac{|H(u,v)|^2}{|H(u,v)|^2 + K} \right] G(u,v)$$

Wiener filter

a b c

FIGURE 5.28 Comparison of inverse and Wiener filtering. (a) Result of full inverse filtering of Fig. 5.25(b). (b) Radially limited inverse filter result. (c) Wiener filter result.

Wiener filter

a b c
d e f
g h i

FIGURE 5.29 (a) 8-bit image corrupted by motion blur and additive noise. (b) Result of inverse filtering. (c) Result of Wiener filtering. (d)–(f) Same sequence, but with noise variance one order of magnitude less. (g)–(i) Same sequence, but noise variance reduced by five orders of magnitude from (a). Note in (h) how the deblurred image is quite visible through a "curtain" of noise.

5. Filters in Fourier space

5.4. Applications

redefine THE POSSIBLE

CT Image Reconstruction

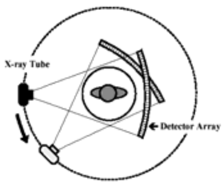

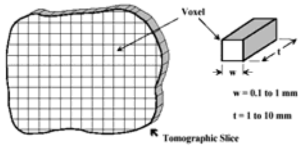

$$ln\left(\frac{I_0}{I_t}\right) = \mu t = \Delta t(\mu_1 + \mu_2 + ... + \mu_n)$$

Back Projection

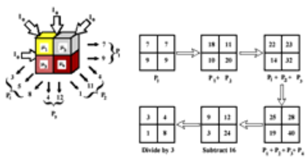

CT Image Reconstruction

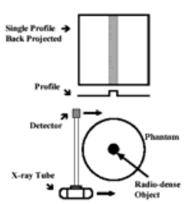

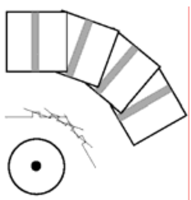

Back Projection

Filtered Back Projection

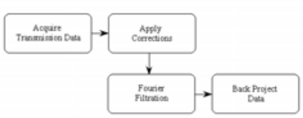

Intensity non-uniformity

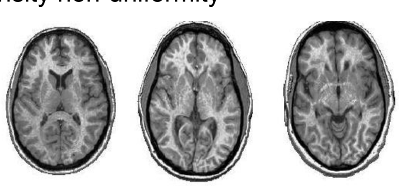

Figure 2.2: T1 weighted brain scans showing diagonal non-uniformity, brighter at the top left and bottom right. The gray scale has been compressed to exaggerate the intensity variations.

- Intensity non-uniformity, “bias” field, shading artifacts, RF inhomogeneity…
- Spatial variation of the image signal unrelated to anatomic information

Causes and effect

Major factors:
- Non-uniform reception sensitivity (multiplicative field, slow varying)
- Inhomogeneity of RF excitation (non-multiplicative field; acquisition)
- RF penetration and standing wave effects (image acquisition)

Minor factors: **Small; The effect increases with the rapid image acquisition**
- eddy currents driven by the switching of field gradients
- Mis-tuning of the RF coil
- Bandwidth filtering of the data
- Geometric distortion (negligible, 1%)

} **Automatically done by scanners**

Effects

- Cause 10% - 30% variation of intensity.
- Reduce accuracy of tissue segmentation, brain-surface extraction
- The higher the field strength, the prominent the intensity non-uniformity

Non-uniformity correction Methods (N3 Method)

IEEE TRANSACTIONS ON MEDICAL IMAGING, VOL. 17, NO. 1, FEBRUARY 1998 87

A Nonparametric Method for Automatic Correction of Intensity Nonuniformity in MRI Data

John G. Sled,* Alex P. Zijdenbos, *Member, IEEE*, and Alan C. Evans

Assumptions and Tasks

Assumption

- Bias field varies smoothly across images
- Model of intensity non-uniformity as a multiplicative field corrupting the measured intensities

Tasks

- To estimate the bias field and true tissue intensity distribution
- To remove the bias field

Overview of Methods

Analytic modeling (too simple, impractical)
Adjust acquisition protocols
Data-driven post-processing:

use filter to estimate a multiplicative non-uniformity field & divide it from the image

eliminate the low frequency components of anatomy when estimating non- uniformity (tissue intensity, spatial homogeneity, field based models)

Overview of the N3 method

Nonuniformity Model

Smooth multiplicative field

$$v(\mathbf{x}) = u(\mathbf{x}) f(\mathbf{x}) + n(\mathbf{x})$$

measured **true?** **bias field?** **white noise?**

Noise issue

$$v(\mathbf{x}) = u(\mathbf{x}) f(\mathbf{x}) + n(\mathbf{x})$$

Filtering

$$v(\mathbf{x}) = u(\mathbf{x}) f(\mathbf{x})$$

Correction

Overview of the N3 method

$$\hat{v}(\mathbf{x}) = \hat{u}(\mathbf{x}) + \hat{f}(\mathbf{x}) \qquad \hat{u}(\mathbf{x}) = \log(u(\mathbf{x}))$$

Let U, V, and F be the probability densities of û, v̂, and $\hat{f}$ respectively.

$V(\hat{v}) = F(\hat{v}) * U(\hat{v})$

Non-uniformity distribution F blurs the histogram of the data U

The task is to restore U by sharpening V

Estimating F

$$V(\hat{v}) = F(\hat{v}) * U(\hat{v})$$

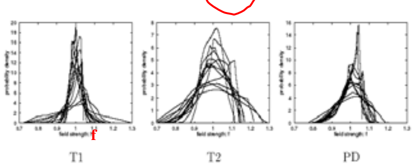

Figure 4.1: Probability densities for non-uniformity fields estimated from white matter on MR scans of twelve individuals taken with twelve different MR scanners. Note that these are the distributions of the dimensionless scale factors f rather than the log of these values $\hat{f}$. The T1 scan is a gradient echo 3D acquisition with TE = 11 ms and TR = 35 ms, while the proton density (PD) and T2 scans are two echoes TE = 30 ms and TE = 80 ms of a multi-slice spin echo acquisition with TR = 3 s.

Estimating F

$$V(\hat{v}) = F(\hat{v}) * U(\hat{v})$$

- Assume that the distribution of F is Gaussian
- Searching an optimal U by finding a Gaussian distributed F having zero mean and given variance
- In other word, the space of all distributions U is collapsed down to a single dimension, the width of the F distribution

85

Fields, 08, HmZhu

Estimating F

$$V(\hat{v}) = F(\hat{v}) * U(\hat{v})$$

- The Gaussian distributed F can be estimated incrementally by convolving narrow Gaussians
- Thus, U can be searched iteratively by deconvolving narrow Gaussians

86

Fields, 08, HmZhu

Estimating U

$$V(\hat{v}) = F(\hat{v}) \otimes U(\hat{v})$$

FT

$$\tilde{V}(k) = \tilde{F}(k) \bullet \tilde{U}(k)$$

$$\tilde{U} = \frac{\tilde{F}^*}{|\tilde{F}|^2 + Z^2} \tilde{V}$$

De-convolution

Constant term to avoid zero division

87

Fields, 08, HmZhu

Estimating the log field $\hat{f}_e$

- Given the distributions F and U, estimate the corresponding field $\hat{f}_e$ at a given single measurement $\hat{v}$

- We assume that the field is smooth. Therefore, we smooth it to obtain an estimated field based on all of the measurements in a neighborhood location x

- Correct the original image $\hat{v}_{new}(\mathbf{x}) = \hat{v}_{old}(\mathbf{x}) - \hat{f}_s(\hat{v}(\mathbf{x}))$

N3 Algorithm

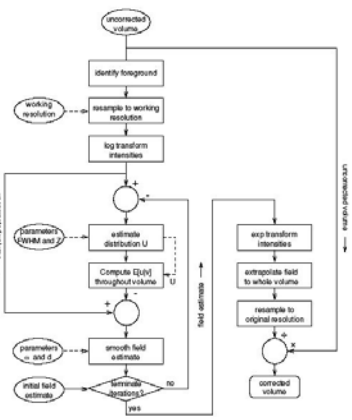

3D volume example 1

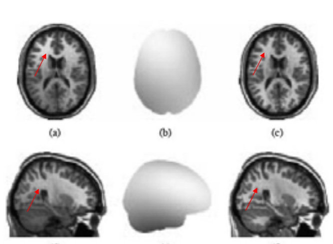

Fig. 12 Intensity nonuniformity correction of a T1 weighted 27-scan averaged gradient-echo MR scan: (a) and (d) transaxial and sagittal views of uncorrected data; (b) and (e) nonuniformity field estimated by the N3 method; (c) and (f) corrected data.

YORK U UNIVERSITÉ UNIVERSITY

3D volume example 2

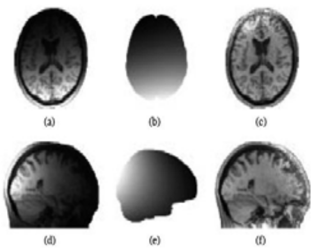

Fig. 13. Intensity nonuniformity correction of a surface coil MR scan: (a) and (d) transaxial and sagittal views of uncorrected data; (b) and (e) nonuniformity field estimated by the N3 method; (c) and (f) corrected data.

Fields, 08, HmZhu

91